Available online at www.sciencedirect.com
SCIENCE DIRECT
Journal of Photochemistry and Photobiology A: Chemistry 166 (2004) 135–140
Journal of Photochemistry and Photobiology A:Chemistry
www.elsevier.com/locate/jphotochem

Fabrication of beam homogenizers in quartz by laser micromachining

G. Kopitkovas [a], T. Lippert [a,*], C. David [b], S. Canulescu [a], A. Wokaun [a], J. Gobrecht [b]

[a] General Energy Research Department, Paul Scherrer Institut, CH-5232 Villigen-PSI, Switzerland
[b] Laboratory for Micro- and Nanotechnology, Paul Scherrer Institut, CH-5232 Villigen-PSI, Switzerland

Abstract

The combination of gray tone phase masks with a laser-based wet etching process can be applied as a one step micromachining process. This technique utilizes a XeCl excimer laser and an absorbing liquid which is in contact with quartz. Microstructures with continuous profiles, such as plano-convex microlenses in quartz, can be created with laser fluence well below the damage threshold of quartz. The roughness of the etched features varies from several micrometers to below 10 nm, depending on the laser fluence and applied absorbing solution. The etch rates of quartz using different organic solutions such as pyrene in acetone or pyrene in tetrahydrofurane reveal a complex behavior, suggesting that several processes dominate at various laser fluences.
© 2004 Elsevier B.V. All rights reserved.

Keywords: Wet etching; Microlens; Homogenizer; Quartz; Laser ablation

1. Introduction

Fused silica is one of the most widely used materials in optics, due to its transparency over a wide wavelength range, strong damage resistance for laser irradiation, and good thermal and chemical stability. Arrays of micro-optical components, such as plano-convex or Fresnel lenses are usually used as beam homogenizers for high power lasers. Homogenization of the laser beam intensity is usually achieved using these optical elements, either in the form of microlens arrays [1] or a random phase plate (RPP) [2,3], in combination with a plano-convex lens. The homogenization of the beam intensity is obtained at the focus of the field lens originating from the superposition of the beams from each individual lens of the array [4]. The conventional method for the fabrication of microstructures with continuous profiles in quartz is photolithography followed by the subsequent transfer of the resist profile into the substrate by reactive ion etching [5]. However, this technique requires excellent control of the exposure dose, resist characteristics, and the proportional etching process. Quartz can be also structured by vacuum UV lasers (VUV) [6] or by utilizing ultrafast lasers [7]. The VUV lasers require an experimental setup where vacuum or an inert gas is used in the beam path, and expensive VUV transparent focusing optics. The femtosecond laser micromachining process is a slow process, which consist of a sequential scanning technique [7].

Yabe and coworkers have developed and investigated a method for micromachining of fused silica and other UV transparent materials, such as CaF_2, and sapphire [8–13] using standard excimer lasers. This one step micromachining technique, named laser induced backside wet etching (LIBWE), allows precise structuring of UV transparent materials with laser fluences well bellow the ablation or damage threshold of the UV transparent dielectrics. The idea behind this method is based on the strong absorption of the laser light by an organic solution which is in contact with the UV transparent dielectric material. The vibrational relaxation of a dye molecules generates a temperature jump [14] at the solid–liquid interface, which results in softening or melting of the UV transparent dielectric glasses and evaporation of the solvent. The evaporation of the solvent forms a bubble which expands rapidly and collapses after a certain time. This collapse creates a pressure jump which may play an important role in the etching of the UV transparent materials by LIBWE. A different approach for the fabrication of three-dimensional microstructures with continuous profiles (such as Fresnel type microlenses) in polymers was developed by David et al. [15]. The key element for this process is a diffractive gray tone phase mask (DGTPM) which is applied to modulate the incoming laser beam intensity. The modulated beam intensity is projected onto the polymer surface where the three-dimensional structures are formed by direct laser ablation. The combination of LIBWE with the projection of a DGTPM opens a new way to fabricate well defined three-dimensional structures with continuous profiles in quartz and in other brittle dielectric materials, such

* Corresponding author. Tel.: +41-56-310-4076; fax: +41-56-310-2688.
E-mail address: thomas.lippert@psi.ch (T. Lippert).

1010-6030/$ – see front matter © 2004 Elsevier B.V. All rights reserved.
doi:10.1016/j.jphotochem.2004.05.001

as CaF_2 [16,17]. Here we report etching of quartz with the solutions of pyrene in acetone and pyrene in tetrahydrofurane (THF). The thermodynamical properties (such as boiling point, heat capacity) of acetone and THF are comparable, but the solubility of pyrene is much higher in THF than in acetone. A random phase plate and array of micro-lenses fabricated in quartz by LIBWE were tested as beam homogenizers for a high power quadrupled Nd:YAG.

2. Experimental

Quartz plates with a thickness of 0.5 mm and surface roughness of about 5 nm were used as samples. A XeCl excimer laser (308 nm, FHWM 30 ns, Lambda Physics) was applied as irradiation source. The laser beam intensity was controlled by a computer controlled attenuator. The repetition rate of the laser was 4 Hz. Several organic solutions were used as etching media, i.e. pyrene in acetone with a concentrations of 0.2 and 0.4 M and pyrene in tetrahydrofurane with a concentration of 0.4–1 M pyrene. One side of the quartz was in contact with the solution while the irradiation was performed through the other side, as shown in Fig. 1. The diffractive gray tone phase masks (DGTPM's) were fabricated by e-beam lithography and reactive ion etching [15]. A refractive doublet lens (10× or 20× demagnification) was used for transferring the image of the DGTPM into the quartz. The etching of the microstructures with continuous profiles was carried out with the variable incident laser fluence from 1.3 to 2.6 J cm^{-2}, which was modulated by the DGTPM, and 80 pulses. The area of the etched features in quartz was 0.5 mm × 0.5 mm. The depth profiles of the etched areas in quartz were measured with a profilometer (DEKTAK 8000).

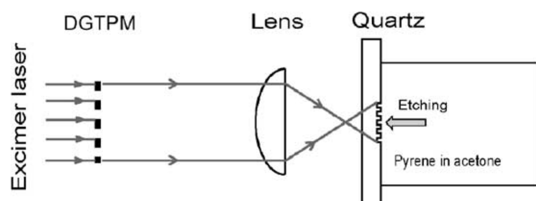

Fig. 1. Scheme of the experimental setup for the fabrication of micro-optical elements in quartz.

3. Results and discussion

The etching of quartz by LIBWE shows a behavior similar to conventional laser ablation, where a threshold fluence exists and below this threshold no etching occurs. The threshold fluences for quartz at different pyrene in acetone and pyrene in THF concentrations are obtained experimentally by measuring etch rates at various laser fluences (shown in Fig. 2A and B). The thresholds for quartz using different etching media (pyrene in acetone and pyrene in THF) and different concentrations of pyrene are summarized in Table 1. The two different threshold fluences in the table correspond to different etching processes, which occur at different fluence ranges. At low laser fluences the etching of quartz did not start with the first laser pulse. This behavior is usually termed incubation, which is described in more detail below. The threshold fluence without incubation is defined as the fluence, above which the etching of quartz starts with the first laser pulse. These fluences were determined from measurements of the etch depth as a function of the pulse number [17]. The threshold fluences without incubation are higher compared to the thresholds determined for etching including incubation. This suggest that different processes dominate in the different fluence ranges (marked as 1 for incubation and 2 without incubation in Fig. 2A and B), as described in detail below. The decreasing thresholds and increasing higher etch rates of quartz (Table 1 and shown in Fig. 2A and B) for different concentration of pyrene in acetone and THF can be explained by an increase of the laser

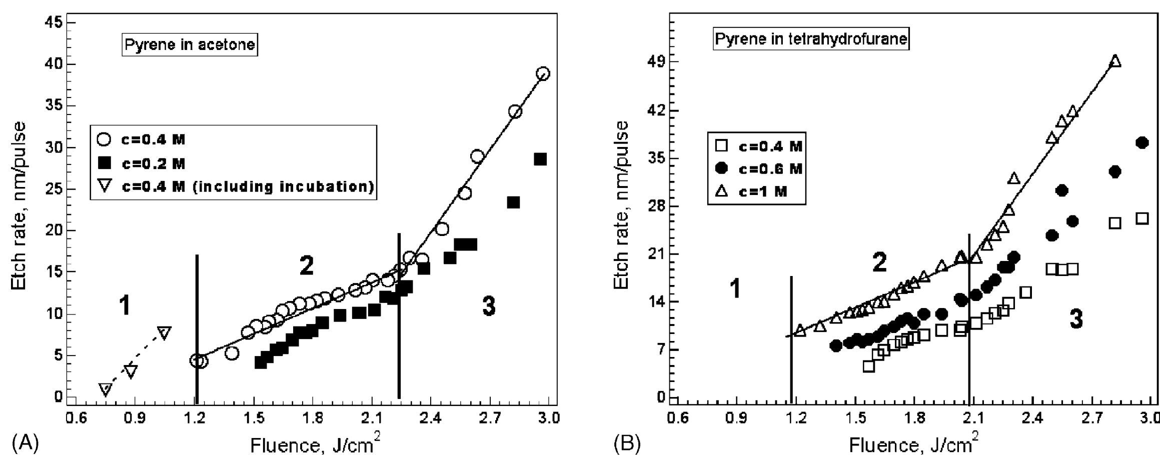

Fig. 2. Etch rate vs. laser fluence using a pyrene–acetone solution (A) and a pyrene–THF solution (B) as etching media. Number of incubation pulses at given fluences for 0.4 M pyrene in acetone solution: 0.75 J cm^{-2}, 1000 pulses; 0.88 J cm^{-2}, 800 pulses; 1.05 J cm^{-2}, 250 pulses.

Table 1
The etching thresholds for quartz using different etching media (pyrene in acetone and pyrene in THF) and different concentrations of pyrene

Concentration of pyrene (M)	Threshold fluence without incubation ($J\,cm^{-2}$)	Threshold fluence with incubation, F_{inc} ($J\,cm^{-2}$)
Pyrene in acetone		
0.2	1.4	
0.4	1.2	0.7
Pyrene in THF		
0.4	1.5	
0.6	1.3	
1	1.1	

induced temperature (as shown in Fig. 3 for the pyrene in acetone case) with increasing pyrene concentration resulting in a thinner absorption layer at the quartz–liquid interface. The different etch rates for pyrene in acetone compared to the same concentration of pyrene in THF may be explained by the fact that acetone has an absorption at the applied laser wavelength while THF is transparent. The nonradiative relaxation of the excited pyrene molecules generates a temperature jump, which results in softening of the quartz. The next step after softening/melting of quartz is the removal of the quartz. A possible mechanism for the removal of the molten quartz from the surface is based on the fact that the laser induced temperature exceed the critical point of the solvent (around 400 K for acetone), which results in boiling of the liquid. The evaporation of the solvent forms a bubble, which expands rapidly, followed by an collapse after a certain time [20]. The pressure wave created by the bubble collapsing may remove the molten quartz by mechanical force [21]. The described etching process may be different at high fluences (shown as a fluence range 3 in Fig. 2A and B). Here, the laser induced temperature (which is shown in Fig. 3) calculated by a model from Fukumura and Masuhara [14], is very high and the etching in this fluence range may be assisted by the creation of a plasma. Plasma etching of the fused silica has been reported previously [22]. This may

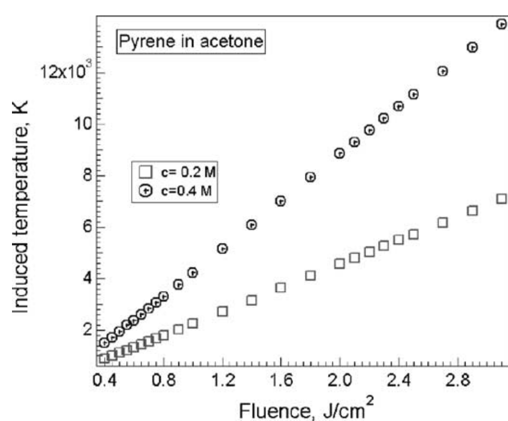

Fig. 3. Calculated temperature jump at the quartz–liquid interface using a pyrene in acetone solution.

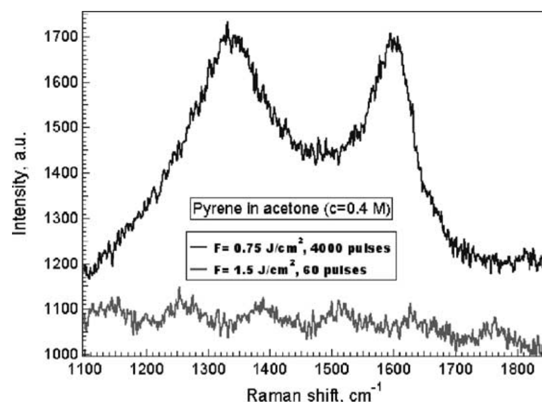

Fig. 4. Raman spectra of the carbon deposits in the etched areas. Spectra are shown for low fluences (0.75 $J\,cm^{-2}$), where the incubation is observed and for the high fluences (1.5 $J\,cm^{-2}$) where no incubation is observed.

also explain the strong increase of the etch rate. Another process is observed in the low laser fluence range, where incubation [9,11,12,17,18] is observed. The incubation effect corresponds most probably to a more efficient absorption of the laser energy, which may suggest two different processes: (i) an increase of the absorption of the quartz probably due to the creation of color centers [17]; (ii) decomposition of pyrene or the solvent, which results in the formation of carbon that adheres to the quartz surface. The adhesion of black particles in sapphire, which was structured by LIBWE, using pyrene in acetone as etching media, was investigated by Ding et al. [13]. The black particles were also detected for the etching of quartz with pyrene in acetone and were analyzed by confocal Raman spectroscopy. The black deposits (shown in Fig. 4) reveal clearly the D and G band of amorphous carbon [23,24], which is produced by the decomposition of the pyrene and/or acetone molecules [13]. The amorphous carbon on the etched quartz surface areas would be detected only at low laser fluences (shown in Fig. 4), but not for the medium and high fluence rages (2 and 3 in Fig. 2A and B). Our Raman microscopy studies of the carbon deposition shows also, that the carbon has some crystalline features. The experimentally observed etch roughness is quite high at low laser fluences (shown in Fig. 5A and B) for both etching solutions and may be due an etching process that is strongly influenced by the carbon deposits, which can have two different effects: (i) the laser energy is deposited in a thin solid layer which may result in different a temperature transfer mechanisms to the quartz as compared to the pure liquid layer without any carbon deposits at the high fluences; (ii) the carbon layer, which is heated by the laser and the quartz have quite different thermal expansion coefficients, which will result in a mechanical stress [19]. This mechanical stress may contribute to the removing of quartz and results in a higher etch roughness. The lowest roughness (≈10 nm) was detected at an intermediate fluence range (1.3–2.1 $J\,cm^{-2}$) for pyrene in acetone and THF solutions as shown in the inserts of Fig. 5A and

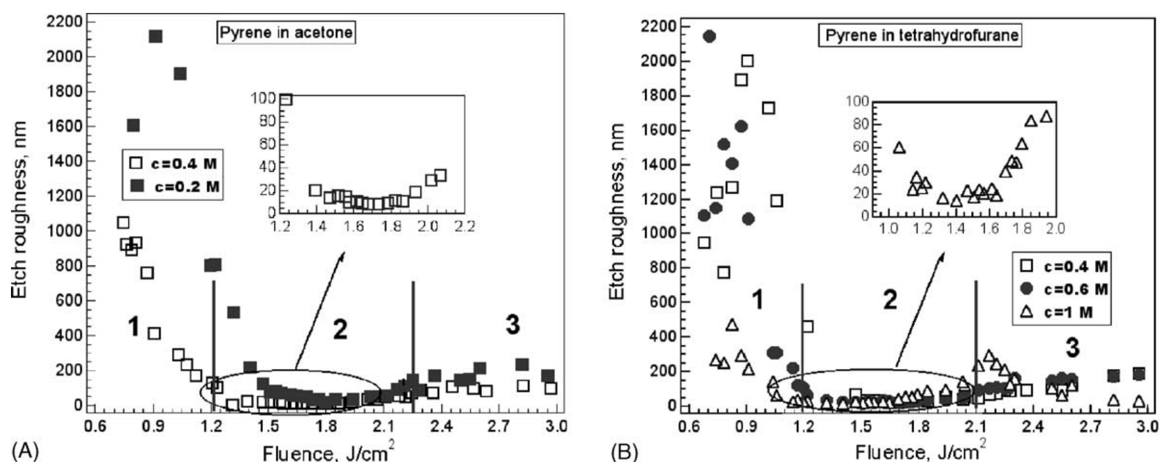

Fig. 5. The roughness of the etched features in quartz: (A) pyrene–acetone solution and (B) a pyrene–THF solution.

B. The combination of the experimental data results in the following scheme of the laser induced backside wet etching (shown in Fig. 6). At laser fluences below the threshold of incubation (where no clear etching is observed even ≥6000 laser pulses are applied) only chemical surface modification are observed. The etching of quartz starts, when the fluence is above the threshold value for incubation (F_{inc}). At the fluences (just above the F_{inc}) the etching of quartz does not starts with the first pulse, but a certain number of "incubation" pulses is required. This suggest that at these fluence range the etching of quartz is influenced either by the decomposition of the solvent and pyrene or by the creation of the defect centers. The etch roughness at these fluences is quite high (several micrometers). When higher fluences are used no incubation and also no carbon is detected in the etched quartz areas. At these fluences (intermediate fluence range) the quartz can be structured with the first laser pulse and the roughness is in the range of ≥10 nm. This clearly indicates a change of the etching mechanism. The slope of the etch rate is again changing when high fluences are applied (>2.3 J cm^{-2}). At this fluence range very high laser-induced temperature jumps may be obtained which may result in the

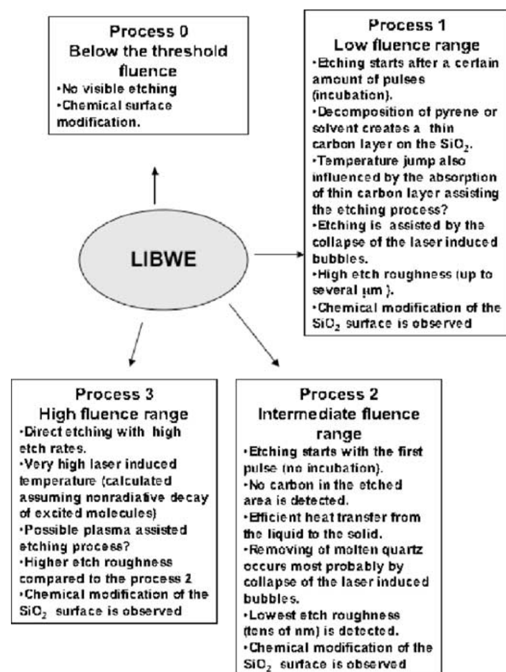

Fig. 6. Possible mechanisms for laser induced backside wet etching of SiO_2 with a pyrene solution.

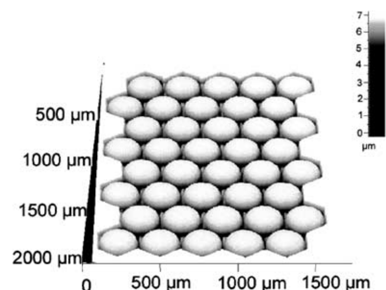

Fig. 7. Three-dimensional scan of a plano-convex microlens array in quartz.

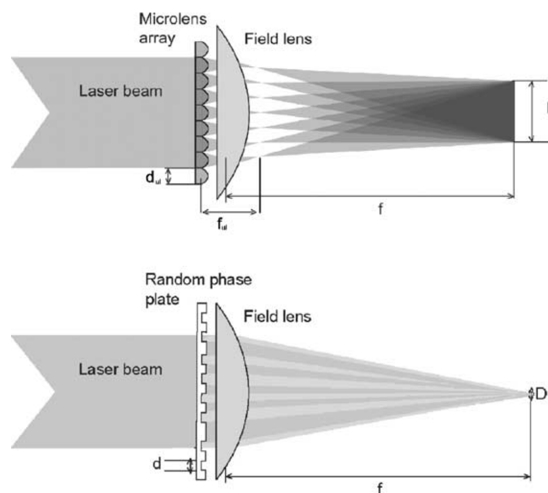

Fig. 8. Scheme of the experimental setup for testing the beam homogenizers.

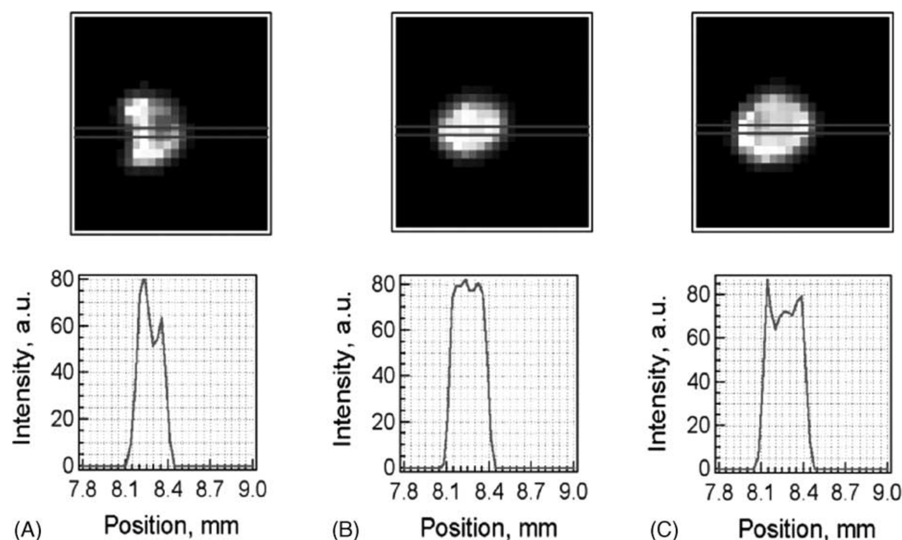

Fig. 9. The beam profile of a quadrupled Nd:YAG laser close to the focal plane of the collecting lens: (A) without the beam homogenizer, (B) with a microlens array and (C) with an RPP.

generation of a plasma in the etching solution. This plasma assists the etching, resulting in the observed high etch rates.

Micro-optical elements in quartz, as discussed above, are very important for homogenizing high power laser beams. Beam homogenizing is based on the idea of splitting the collimated beam into many beamlets, which are superimposed in the focal plane of the field lens. Each microlens acts as a divergent optical element, which homogeneously distributes the inhomogenities of the laser beam intensity over the complete irradiated area. A microlens array was prepared in quartz by using pyrene in THF with a concentration of 1 M as "etchant" and a laser (XeCl) fluence which is modulated with the DGTPM between 1.3 and 2.6 J cm^{-2}. This corresponds to the conditions were the lowest etch roughness over the complete range is obtained. The diameter of a single lens in the plano-convex microlens array in quartz (shown in Fig. 7) is about 270 μm, while the focal length of each lens is 6 mm. Another beam homogenizers type, i.e. random phase plate (RPP) was also fabricated in quartz and tested as an alternative homogenizer for a quadrupled high power Nd:YAG lasers. An RPP consists of a two-dimensional binary array of transmitting areas, where each area induces a randomly phase shift of 0 or π rad. The comparison of the two beam homogenizers was performed by measuring the transmitted beam profile at the focal plane of the field lens, as shown in Fig. 8. The spatial energy distribution close to the focal plane without and with beam homogenizers is shown in Fig. 9. The flat top spatial energy profile, observed with the microlens array (shown in Fig. 9B) shows clearly the best, most homogenous energy distribution. The application of the RPP results also in an improvement of the energy profile (shown in Fig. 9C). The transmission of two homogenizers was also measured and values of 75% for the microlens array and 85% for the random phase plate were obtained.

4. Conclusion

The combination of laser induced backside wet etching and projection of diffractive gray tone phase masks offers the possibility for a fast *one-step* fabrication of three-dimensional objects, e.g. microlens arrays in UV transparent materials. The roughness of the etched features varies between tens of nm to several micrometers, depending on the organic solution and applied laser fluence. Another optical element that has been created by LIBWE in quartz is a random phase plate which is an alternative beam homogenizer for high power lasers. A clear improvement of the energy profile for a quadrupled Nd:YAG laser is obtained with the RPP and the microlens array, but with better results obtained from the microlens array.

Acknowledgements

The authors would like to thank the technical staff of the Laboratory for Micro- and Nanotechnology and for the excellent working conditions. Financially support by PSI is gratefully acknowledged.

References

[1] C. Kopp, L. Ravel, P. Meyrueis, J. Opt. A: Pure Appl. Opt. 1 (1999) 398–403.
[2] Y. Kato, K. Mima, N. Miyanaga, S. Arinaga, Y. Katigawa, H. Nakatsuka, C. Yamanaka, Phys. Rev. Lett. 53 (1984) 1057–1060.
[3] C.S. Lewis, I. Weaver, L.A. Doyle, G.W. Martin, T. Morrow, Rev. Sci. Instrum. 70 (1999) 2116–2120.
[4] O. Homburg, B. Finke, P. Harten, L. Lissotsenko, EuroPhotonics 7 (2003) 34–35.
[5] S. Sinzinger, J. Jahns, Microoptics, 2nd ed., Wiley/VHC GmbH, Germany, 2003.

[6] J. Ihlemann, S. Müller, S. Pouchmann, D. Schäfer, M. Wei, J. Li, P.R. Herman, Appl. Phys. A 76 (2003) 751–753.
[7] A. Marcinkevicius, S. Juodkazis, M. Watanabe, H. Miwa, S. Matsuo, H. Misawa, J. Nishii, Opt. Lett. 36 (2001) 277–279.
[8] J. Wang, H. Niino, A. Yabe, Appl. Surf. Sci. 154–155 (2000) 571–576.
[9] X. Ding, Y. Yasui, Y. Kawaguchi, H. Niino, A. Yabe, Appl. Phys. A 75 (2002) 437–440.
[10] X. Ding, Y. Yasui, Y. Kawaguchi, H. Niino, A. Yabe, Appl. Phys. A 75 (2002) 641–645.
[11] H. Niino, Y. Yasui, X. Ding, A. Narazaki, T. Sato, Y. Kawaguchi, A. Yabe, J. Appl. Photochem. Photobiol. A 158 (2003) 179–182.
[12] Y. Yasui, H. Niino, Y. Kawaguchi, A. Yabe, Appl. Surf. Sci. 186 (2002) 552–555.
[13] X. Ding, T. Sato, Y. Kawaguchi, H. Niino, Jpn. J. Appl. Phys. 42 (2003) 176–178.
[14] H. Fukumura, H. Masuhara, Chem. Phys. Lett. 221 (1994) 373–378.
[15] C. David, T. Lippert, J. Wei, A. Wokaun, Microelectr. Eng. 57–58 (2001) 453–460.
[16] G. Kopitkovas, T. Lippert, C. David, A. Wokaun, J. Gobrecht, Microelectr. Eng. 67–68 (2003) 438–444.
[17] G. Kopitkovas, T. Lippert, C. David, A. Wokaun, J. Gobrecht, Thin Solid Films 453–454 (2004) 31–35.
[18] K. Zimmer, A. Braun, R. Böhme, Appl. Surf. Sci. 9594 (2003) 1–6.
[19] A.V. Simakin, E.N. Lubnin, G.A. Shafeev, Quant. Electron. 30 (2000) 263–267.
[20] J.C. Isselin, A.P. Allonce, M. Autric, J. Appl. Phys. 84 (1998) 5766–5771.
[21] Y. Kawaguchi, X. Ding, A. Narazaki, T. Sato, H. Niino, Appl. Phys. A (2004) in press.
[22] K. Sugioka, K. Obata, M.H. Hong, D.J. Wu, L.L. Wong, Y.F. Lu, T.C. Chong, K. Midorikawa, Appl. Phys. A 77 (2003) 251–257.
[23] S. Diane, S. Knight, W.B. White, J. Mater. Res. 4 (1989) 385–393.
[24] F. Raimondi, S. Abolhassani, R. Brütsch, F. Geiger, T. Lippert, J. Wambech, J. Wei, A. Wokaun, J. Appl. Phys. 88 (2000) 3659–3666.